CONFIDENTIAL

Copy 6
RM L50K15

NACA RM L50K15

NACA

UNCLASSIFIED

RESEARCH MEMORANDUM

LONGITUDINAL-CONTROL EFFECTIVENESS AND DOWNWASH CHARACTERISTICS AT A MACH NUMBER OF 1.24 OF A $\frac{1}{30}$-SCALE SEMISPAN MODEL OF THE BELL X-5 AIRPLANE AS DETERMINED BY THE NACA WING-FLOW METHOD

By Richard H. Sawyer, Robert M. Kennedy,
and Garland J. Morris

Langley Aeronautical Laboratory
Langley Field, Va.

CLASSIFICATION CANCELLED

Authority .... Date ....

By .... See ....

NATIONAL ADVISORY COMMITTEE
FOR AERONAUTICS

WASHINGTON

January 8, 1951

CONFIDENTIAL

UNCLASSIFIED

NACA RM L50K15

NATIONAL ADVISORY COMMITTEE FOR AERONAUTICS

RESEARCH MEMORANDUM

LONGITUDINAL-CONTROL EFFECTIVENESS AND DOWNWASH CHARACTERISTICS AT A MACH NUMBER OF 1.24 OF A $\frac{1}{30}$-SCALE SEMISPAN MODEL OF THE BELL X-5 AIRPLANE AS DETERMINED BY THE NACA WING-FLOW METHOD

By Richard H. Sawyer, Robert M. Kennedy,
and Garland J. Morris

SUMMARY

An investigation was made at a Mach number of 1.24 by the NACA wing-flow method to determine the longitudinal-control effectiveness and downwash characteristics of a $\frac{1}{30}$-scale semispan model of the variable-sweep Bell X-5 airplane with the wing of the model swept back 60°, 50°, and 40°. Lift, drag, and pitching moments were obtained for various angles of attack for several horizontal tail settings and with tail off for each angle of sweep of the wing. The Reynolds number was about 1×10^6.

The results of the investigation indicated that the rate of change of pitching-moment coefficient with tail incidence was apparently unaffected within the accuracy of measurement by the sweepback of the wing of the model and had a constant value of about -0.016 per degree over the range of angle of attack covered (-2° to 6°). The downwash results computed from the measurements of pitching moment with tail on and tail off resulted in a value of 0.38 for the average rate of change of downwash angle with angle of attack for the model with the wing swept back 60° over the range of angle of attack covered (-2° to 8°). The rate of change of downwash angle with angle of attack appeared to have approximately the same value for the model with the wing swept back 50° and 40° as was determined for the model with the wing swept back 60°.

INTRODUCTION

As part of a program to determine the aerodynamic characteristics of the proposed Bell X-5 airplane incorporating a wing whose angle of sweep can be varied in flight, an investigation is being made at low supersonic speeds by the NACA wing-flow method on a $\frac{1}{30}$-scale semispan model. Results of tests to determine the longitudinal stability characteristics of this model with the wing swept back 60° have been reported in reference 1, and results of tests to determine the effect of sweepback on the longitudinal stability characteristics of this model have been reported in reference 2. The present paper give the results of tests which, when combined with the results previously reported, are used to determine the longitudinal-control effectiveness and downwash characteristics of the model. The results presented herein consist of measurements of lift, drag, and pitching moment for the model with tail incidences of 0° and -4° with the wing swept back 60° and a tail incidence of -2° with the wing swept back 50° and 40°. Measurements were also made for each sweepback angle with the tail off. The effective Mach number at the wing of the model for the tests was about 1.24 and the Reynolds number was of the order of 1×10^6.

In the interest of making these data available as soon as possible, they are presented with only a limited analysis.

SYMBOLS

b wing span, inches

c local wing chord parallel to plane of symmetry, (portion of wing within fuselage is considered to be formed by perpendiculars from wing-fuselage intersections to plane of symmetry), inches

$\bar{c}$ mean aerodynamic chord of wing, inches; based on the relationship

$$\frac{\int_0^{b/2} c^2 dy}{\int_0^{b/2} c\, dy}$$

$\bar{c}_t$ mean aerodynamic chord of tail, inches

[redacted]

C_D drag coefficient (D/qS)

$C_{D_{C_{L=0}}}$ drag coefficient at zero lift

C_L lift coefficient (L/qS)

C_m pitching-moment coefficient $(M/qS\bar{c})$

C_{L_α} rate of change of lift coefficient with angle of attack over linear part of curve

C_{m_α} mean rate of change of pitching-moment coefficient with angle of attack between $\alpha = 0^\circ$ and $\alpha = 6^\circ$

D drag force (resultant force parallel to local free-stream velocity), pounds

$\frac{dC_m}{di_t}$ effectiveness of horizontal tail, per degree

$\frac{d\epsilon}{d\alpha}$ rate of change of downwash with angle of attack at tail of model

i_t incidence of horizontal tail (referred to wing-chord plane), degrees

L lift force (resultant force perpendicular to stream velocity), pounds

M pitching moment, inch-pounds

M_L local Mach number at wing surface of F-51D airplane

M_t effective Mach number for tail of model

M_w effective Mach number for wing of model

q effective dynamic pressure for wing of model, pounds per square foot $(\rho V^2/2)$

R Reynolds number based on mean aerodynamic chord $\bar{c}$

S model wing area, square feet $\left(\int_0^{b/2} c\, dy\right)$

[redacted]

V	velocity, feet per second
y	spanwise coordinate, inches
α	angle of attack (referred to wing-chord plane), degrees
ϵ	effective downwash angle at tail of model, degrees
Λ	sweepback angle referred to 25-percent-chord line
ρ	mass density, slugs per cubic foot

A prime indicates coefficients based on dimensions of configuration with 60° sweptback wing.

APPARATUS AND TESTS

The tests were made by the NACA wing-flow method in which the model is mounted in the region of high-speed flow over the wing of a North American F-51D airplane. The contour of the airplane wing in the test region for the present investigation was designed to give a Mach number of 1.25 at a flight Mach number of about 0.71.

The configurations tested and reported herein consisted of the $\frac{1}{30}$-scale semispan model of the Bell X-5 airplane equipped successively with a 60° sweptback wing for tail incidences of 0° and -4° and with wings of 40° and 50° sweepback angles for a tail incidence of -2°. The model was also tested with tail off for each angle of sweep of the wing.

A photograph of the semispan model with an end plate at the fuselage center line is shown in figure 1; photographs of the model equipped with wings swept back 40° and 50° are shown in figures 2 and 3, respectively. The geometric characteristics of the model, wings, and horizontal tail surfaces are given in table I; other details of the model are shown in figure 4. The fuselage of the model was constructed of mahogany reinforced with duralumin, and duralumin was used for the wings and empennage. A duct was included in the fuselage to simulate to some extent the air intake and flow through the jet engine of the full-scale airplane. The airfoil section perpendicular to the unswept 38-percent-chord line (wing pivot point of the full-scale airplane) is an NACA $64_{(10)}$A011 at the root (through pivot point) and tapers to NACA $64_{(08)}$A008.6 at the tip. The horizontal tail has an NACA 64A006 airfoil section parallel to free stream. The quarter-chord line of the tail was

[redacted]

swept back 45°. The aspect ratios of the 60°, 50°, and 40° wings are 2.18, 2.98, and 3.77, respectively.

The mounting of the model and method of testing were similar to that described in references 1 and 2. The model was originally designed and constructed so that the pitching moment would be measured about the 25-percent mean-aerodynamic-chord position (gross-weight center-of-gravity position of the full-scale airplane) of the wing in each sweep position. However, subsequent changes in wing span and fillets caused the positions about which the pitching moments were measured to correspond to the 26-, 29-, and 35-percent mean aerodynamic chord of the 60°, 50°, and 40° wings, respectively.

A typical chordwise Mach number distribution in the test region on the airplane wing as determined from static-pressure measurements at the wing surface with the model removed is indicated in figure 5. From static-pressure measurements made with a static-pressure tube located at various distances up to 6 inches above the surface of the test section, the average vertical Mach number gradient was found to be 0.009 per inch. The effective dynamic pressure for the model wing q, the effective Mach number for the model wing M_w, and the effective Mach number for the model tail M_t were determined from an integration of the Mach number distribution over the area covered by the wing and tail of the model. A more complete discussion of the method of determining the effective Mach number and dynamic pressure for the model can be found in reference 3. For the present tests, the Mach number for the wing of the model was between 1.23 and 1.24. The Reynolds numbers based on the respective mean aerodynamic chords were about 1.1×10^6 ±9 percent for the 60° wing, 0.9×10^6 ±3 percent for the 50° wing, and 0.9×10^6 ±9 percent for the 40° wing.

RESULTS AND DISCUSSION

The aerodynamic characteristics are presented for the model with the various tail settings and with the tail off in figure 6 for the 60° sweptback wing, in figure 7 for the 50° sweptback wing, and in figure 8 for the 40° sweptback wing. The coefficients of the 60°, 50°, and 40° sweptback wings are based on their respective dimensions. Data are shown for both increasing and decreasing angles of attack obtained as the model was oscillated through a range of angle of attack of about 15°, the limits varying from -2° or -3° to 12° or 13°, depending on the configuration. Pitching-moment data were obtained only over a limited angle-of-attack range for the tests with the tail on because of limitations in the capacity of the pitching-moment element of the balance.

In order to indicate the variation in aerodynamic characteristics with sweep, as for a variable-sweep airplane, lift, drag, and pitching-moment coefficients for the 60°, 50°, and 40° configurations for the various tail settings and for the tail off, all based on the dimensions of the 60° wing, are presented in figures 9, 10, and 11, respectively. The pitching-moment coefficients given in figure 11 refer to the 26-percent mean aerodynamic chord of the 60° wing. Results of tests made with other tail settings are also shown in figures 9, 10, and 11 and are reported in references 1 and 2.

Longitudinal stability characteristics.- The lift and pitching-moment variations with angle of attack and the drag variation with lift given in figures 9 to 11 for the model configurations with tail on of the present tests agreed closely with the results with other tail settings previously reported in references 1 and 2. Figure 12 presents the effect of sweepback angle with tail on and tail off on C_{L_α}, on $C_{D_{C_{L=0}}}$, and on C_{m_α} taken from the results given in figures 9 to 11. As shown in figure 12, the value of C_{L_α} with the tail off was reduced about 0.006 from the value with the tail on for all three sweepback angles of the wing. The value of $C_{D_{C_{L=0}}}$ with the tail off was only slightly less than with the tail on. The contribution of the tail to the stability amounted to about -0.010 in the value of C_{m_α} for all three sweepback angles of the wing.

Longitudinal-control effectiveness.- The effectiveness of the horizontal tail in producing changes in pitching moment is shown in figure 13 at several angles of attack for the model with the 60°, 50°, and 40° sweptback wings. All pitching-moment data shown in figure 13 are based on the dimensions of the model with the 60° sweptback wing. The slope of the variation of pitching-moment coefficient with tail incidence $\frac{dC_m'}{di_t}$, regarded as the tail effectiveness parameter, apparently had a constant value of about -0.016 per degree over the range of angle of attack covered in the tests (-2° to 6°) and appeared to be unaffected within the accuracy of the measurements by sweepback of the wing of the model.

Downwash at the tail.- The downwash angles shown in figure 14 were calculated from the results given in figures 11(a), 11(b), and 11(c) on the basis that the downwash angle was equal to the sum of the tail setting and the angle of attack at which the pitching moment for the particular tail setting was equal to the pitching moment with the tail off. The absolute magnitude of the effective downwash angle determined in this manner is subject to some uncertainty as unpublished results have indicated that there is a variation of approximately 1° in the

direction of flow over the F-51D wing between the positions occupied by the wing and the tail of the model. This curvature of flow is believed to be responsible primarily for the downwash angle not being zero at the angle of attack for zero lift. However, the variation of downwash angle with angle of attack determined by this method should not be affected by this curvature of flow. The results denoted by the flagged symbol were taken from unpublished results of tests of the model with a 60° sweptback wing having approximately one-half the stiffness of the 60° sweptback wing of the present tests. Since it was felt that the difference in stiffness would not materially affect the downwash characteristics, these data were used to aid in defining the variation of downwash angle with angle of attack for the 60° swept wing.

For the model with the 60° swept wing, the rate of change of the downwash angle with angle of attack appeared to average about 0.38 over the angle-of-attack range covered (-2° to 8°). Sufficient data were not obtained with the wings of 40° and 50° sweep to establish adequately the variation of the downwash angle with angle of attack. However, since there is little variation with sweep in the contribution of the tail to the C_{m_α} and since the value of $\frac{dC_m'}{di_t}$ appeared to be constant with sweep (see figs. 12 and 13), the rate of change of downwash angle with angle of attack is probably approximately the same for the model with the wing swept back 50° and 40° as for the model with the wing swept back 60°.

Langley Aeronautical Laboratory
National Advisory Committee for Aeronautics
Langley Field, Va.

REFERENCES

1. Silsby, Norman S., Morris, Garland J., and Kennedy, Robert M.: Longitudinal Characteristics at a Mach Number of 1.24 of $\frac{1}{30}$-Scale Semispan Model of Bell X-5 Variable-Sweep Airplane with Wing Swept Back 60° from Tests by NACA Wing-Flow Method. NACA RM L50E02a, 1950.

2. Morris, Garland J., Kennedy, Robert M., and Silsby, Norman S.: The Effect of Sweepback on the Longitudinal Characteristics at a Mach Number of 1.24 of a $\frac{1}{30}$-Scale Semispan Model of the Bell X-5 Airplane from Tests by the NACA Wing-Flow Method. NACA RM L50I28, 1950.

3. Johnson, Harold I.: Measurements of Aerodynamic Characteristics of a 35° Sweptback NACA 65-009 Airfoil Model with $\frac{1}{4}$-Chord Plain Flap by the NACA Wing-Flow Method. NACA RM L7F13, 1947.

TABLE I

GEOMETRIC CHARACTERISTICS OF $\frac{1}{30}$ - SCALE SEMISPAN MODEL OF

BELL X-5 VARIABLE-SWEEP AIRPLANE

Wing dimensions:			
Airfoil section (perpendicular to unswept 38-percent-chord line)			
Root	NACA $64_{(10)}$A011		
Tip	NACA $64_{(08)}$A008.6		
Sweepback angle, degrees	40	50	60
Semispan, inches	5.31	4.60	3.88
Mean aerodynamic chord, inches	3.10	3.20	3.64
Chord at tip, inches	1.84	1.84	1.84
Chord at plane of symmetry, inches	4.40	4.50	4.25
Area (semispan), square inches	14.97	14.20	13.79
Aspect ratio	3.77	2.98	2.18
Dihedral (chord plane), degrees	0	0	0
Incidence (chord plane), degrees	0	0	0
Horizontal tail:			
Section	NACA 64A006		
Semispan, inches	1.91		
Mean aerodynamic chord, inches	1.43		
Chord at tip, inches	0.72		
Chord at plane of symmetry, inches	1.95		
Area (semispan) square inches	2.55		
Aspect ratio	2.86		
Height (above wing chord), inches	0.56		
Length			
From $0.26\bar{c}$ of 60° swept wing to $0.25\bar{c}_t$, inches	6.83		
From $0.29\bar{c}$ of 50° swept wing to $0.25\bar{c}_t$, inches	6.83		
From $0.35\bar{c}$ of 40° swept wing to $0.25\bar{c}_t$, inches	6.83		

[redacted]

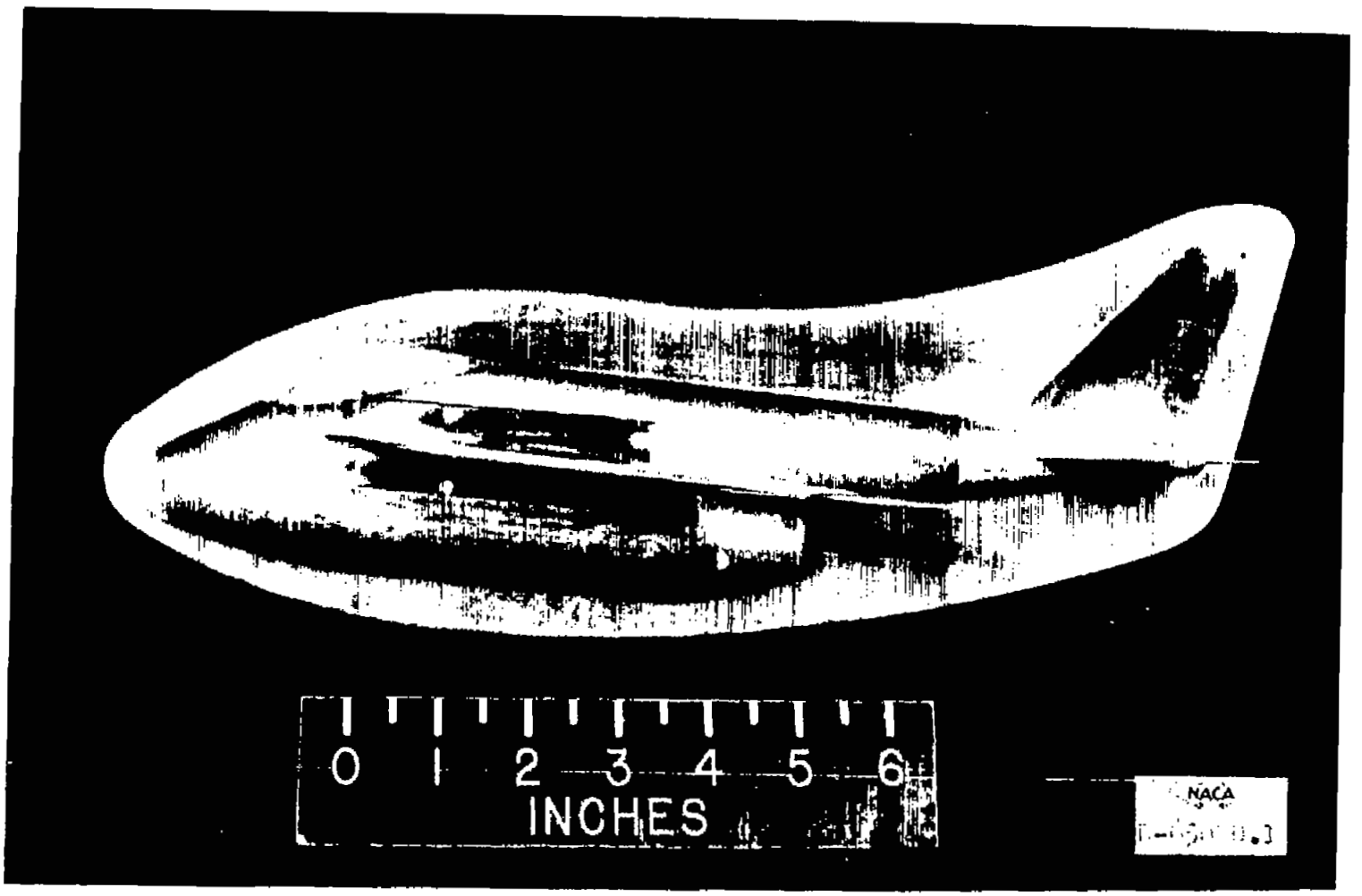

Figure 1.- Side view of semispan wing-flow model of the Bell X-5 airplane.

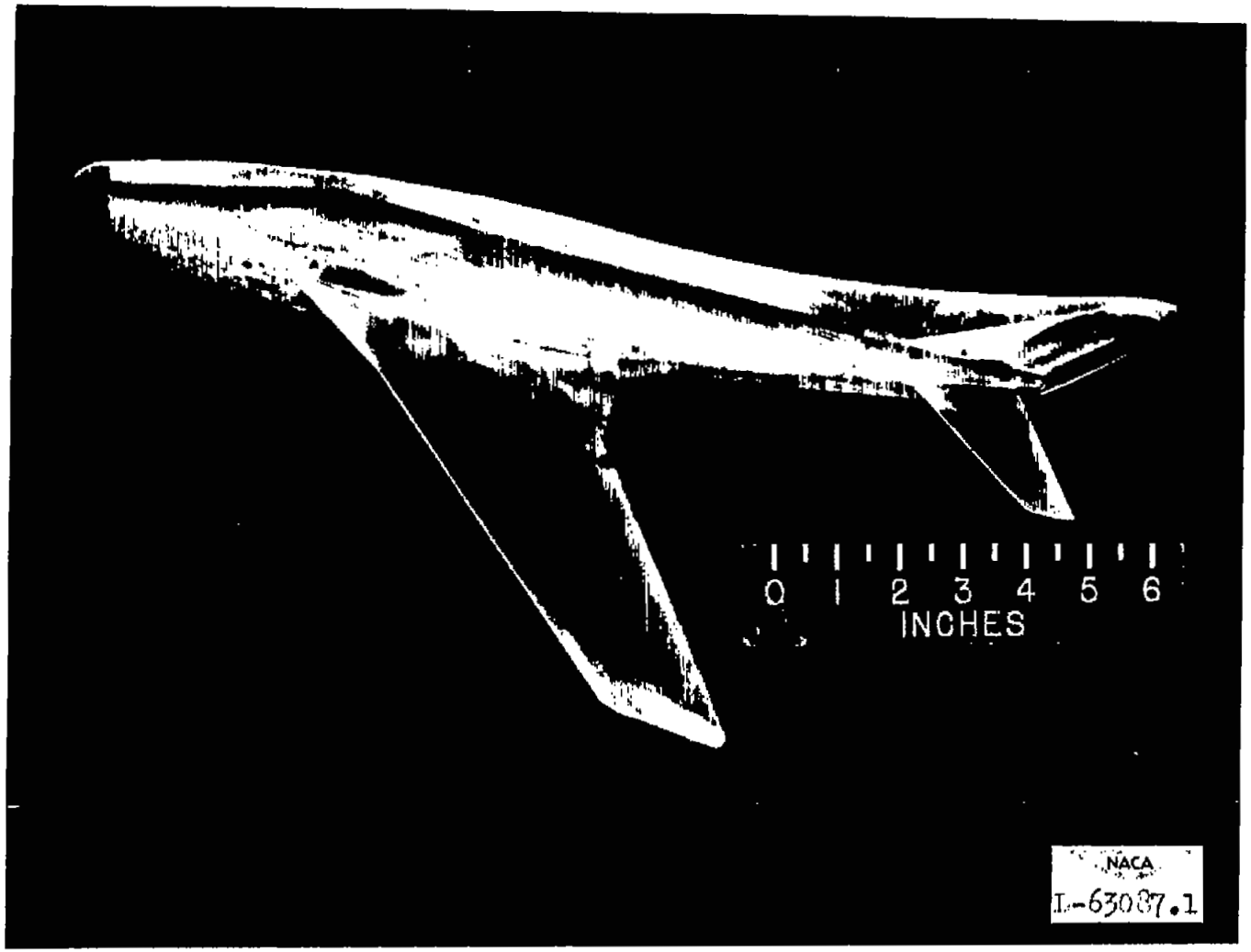

Figure 2.- Semispan wing-flow model of the Bell X-5 airplane with wing in 40° sweep position.

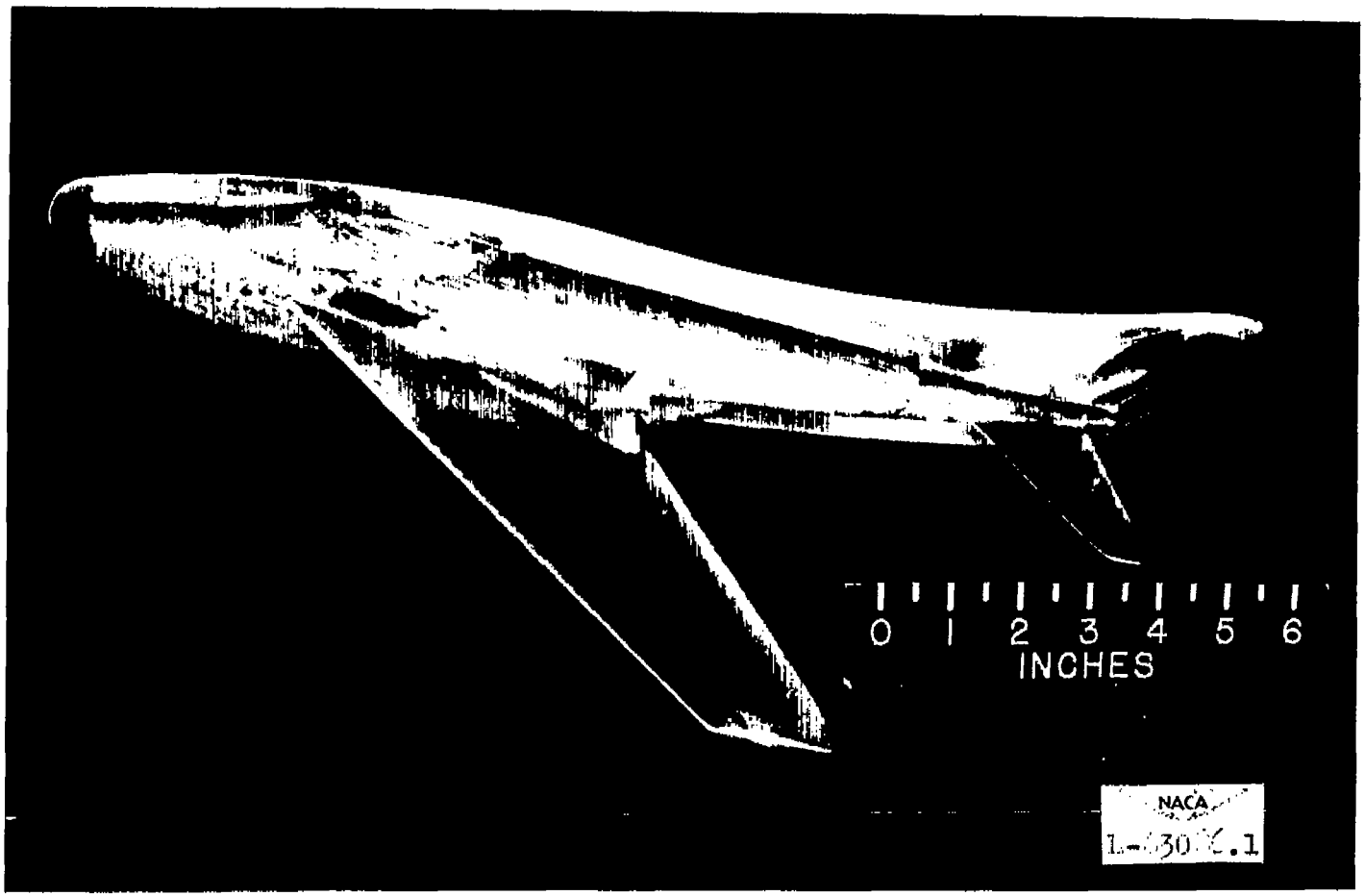

Figure 3.- Semispan wing-flow model of the Bell X-5 airplane with wing in 50° sweep position.

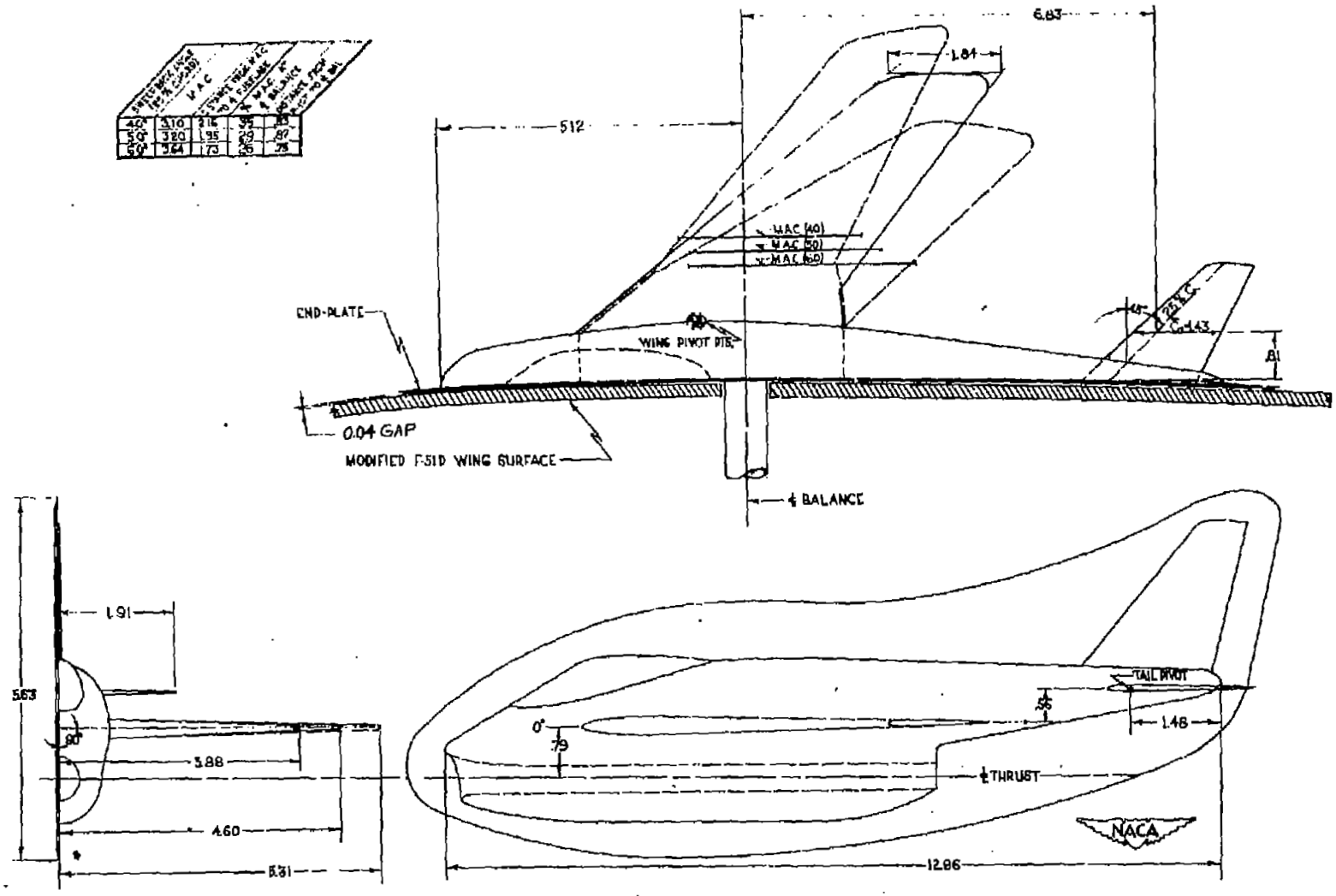

Figure 4.- Details of the semispan model of the Bell X-5 airplane with wing in 40°, 50°, and 60° sweep position. All dimensions are in inches.

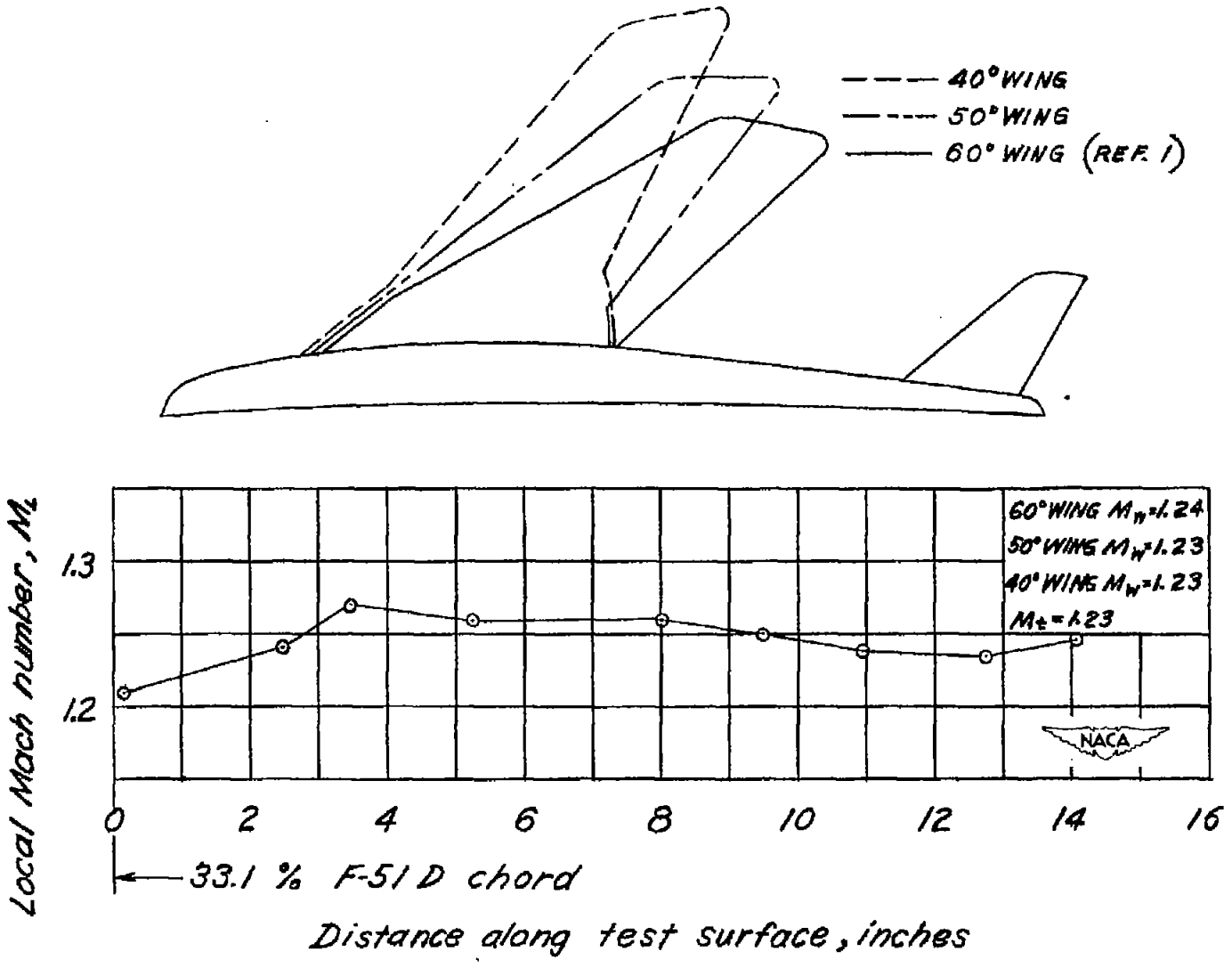

Figure 5.- Typical chordwise distribution of Mach number along the surface of test section. Chordwise location of model also shown.

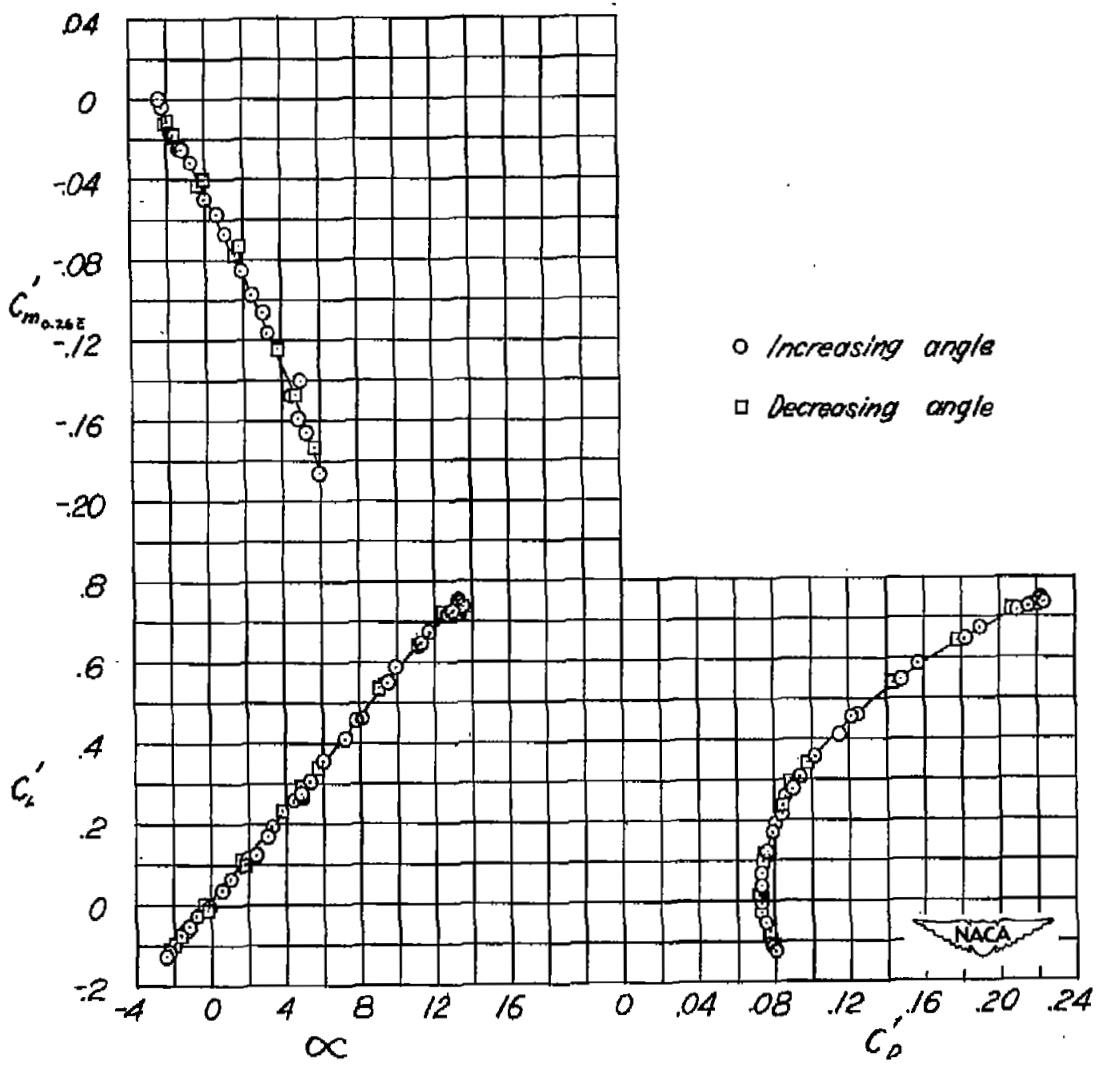

(a) $i_t = 0^\circ$.

Figure 6.- Aerodynamic characteristics of semispan model of Bell X-5 airplane; sweepback angle 60°. $M_w = 1.24$.

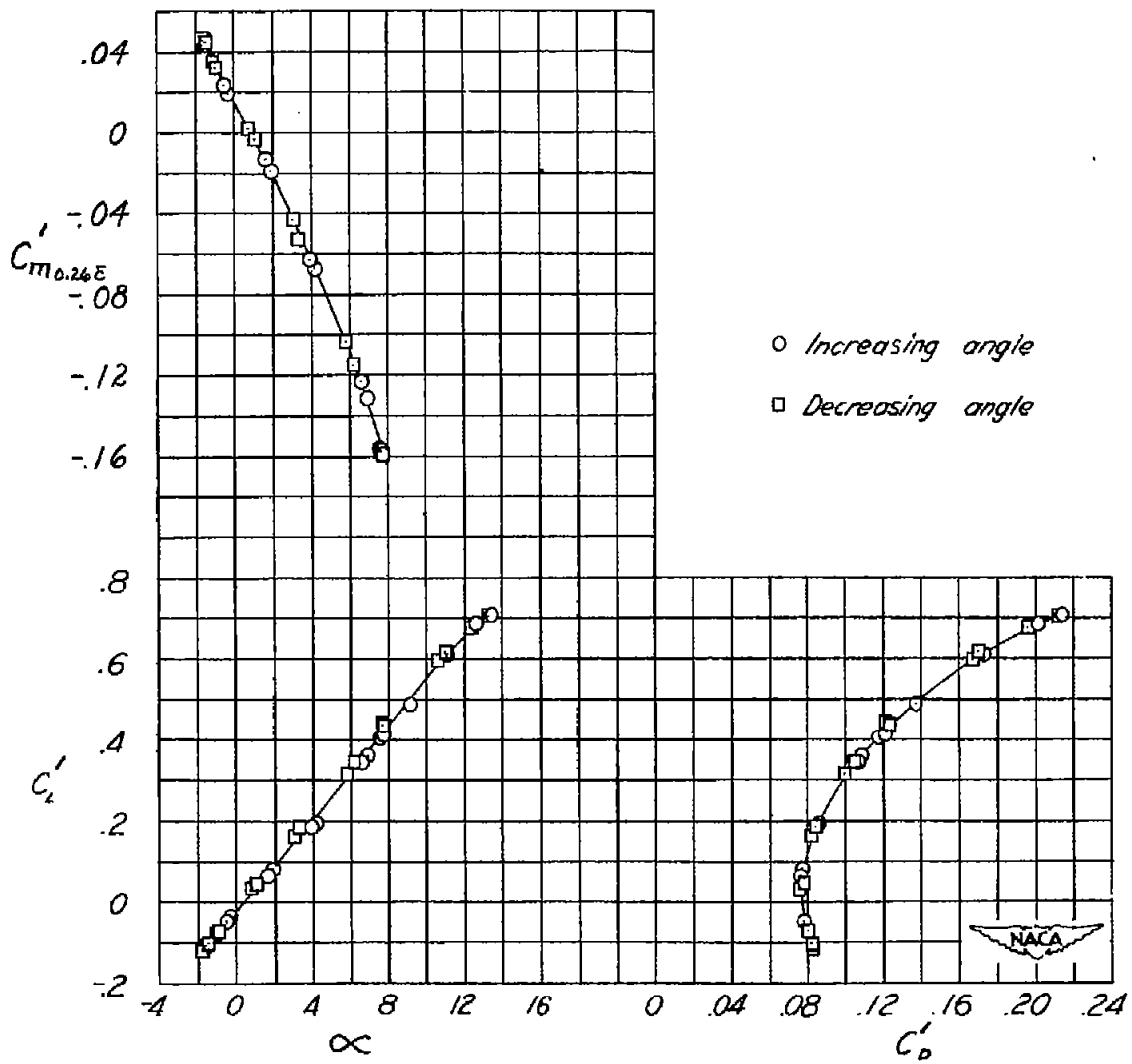

(b) $i_t = -4^\circ$.

Figure 6.- Continued.

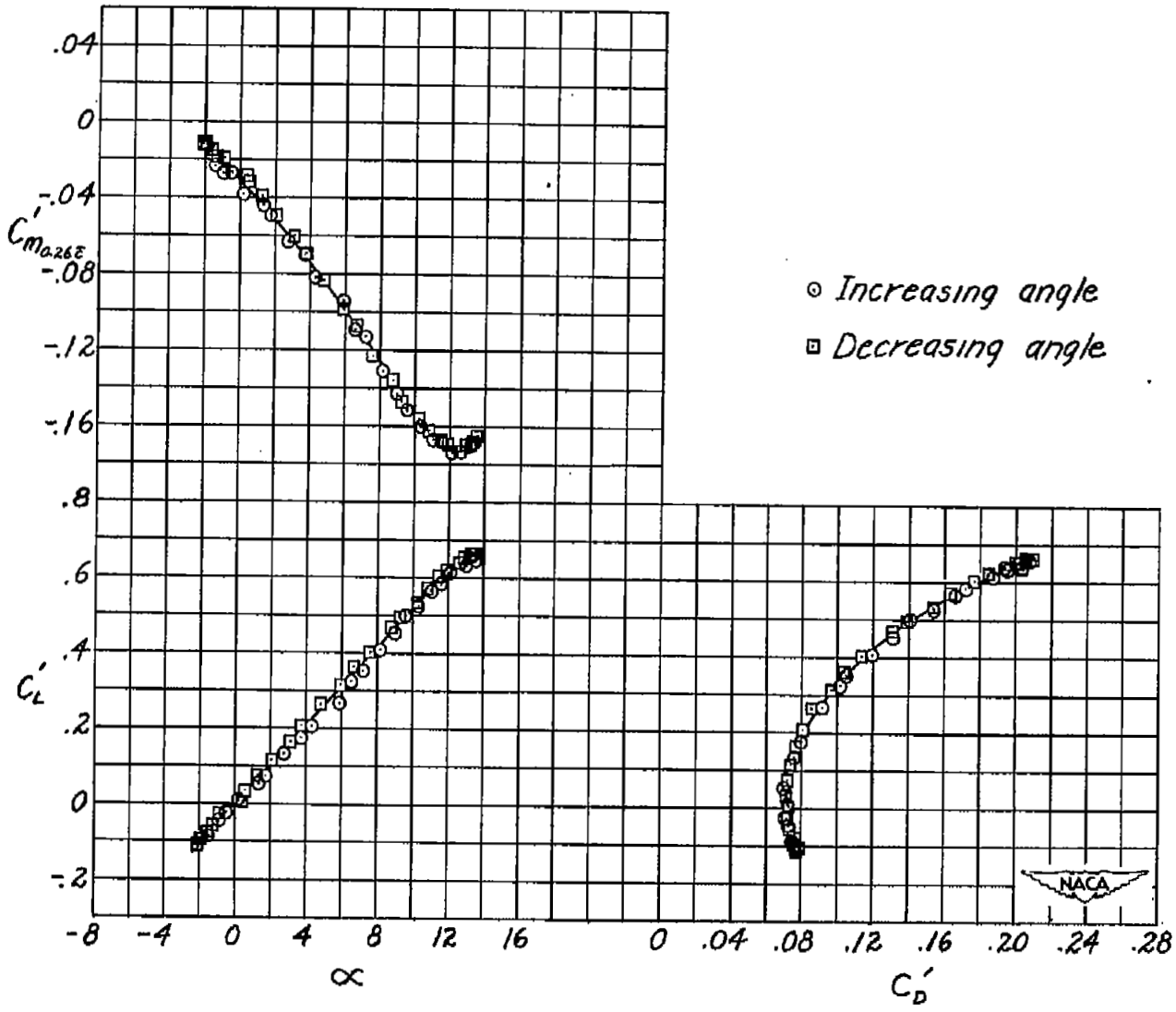

(c) Horizontal tail off.

Figure 6.- Concluded.

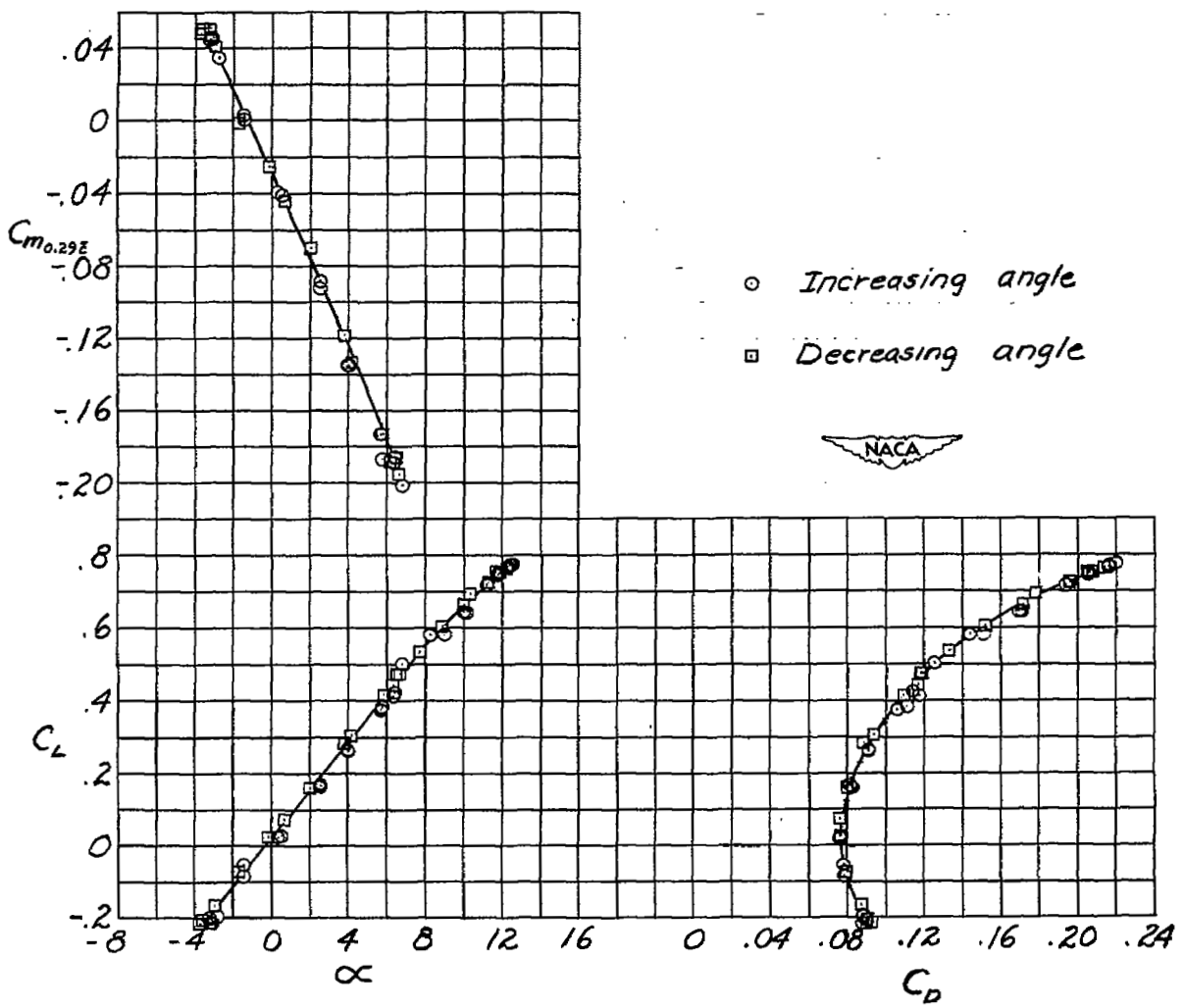

(a) $i_t = -2^\circ$.

Figure 7.- Aerodynamic characteristics of semispan model of Bell X-5 airplane; sweepback angle 50°. $M_w = 1.23$.

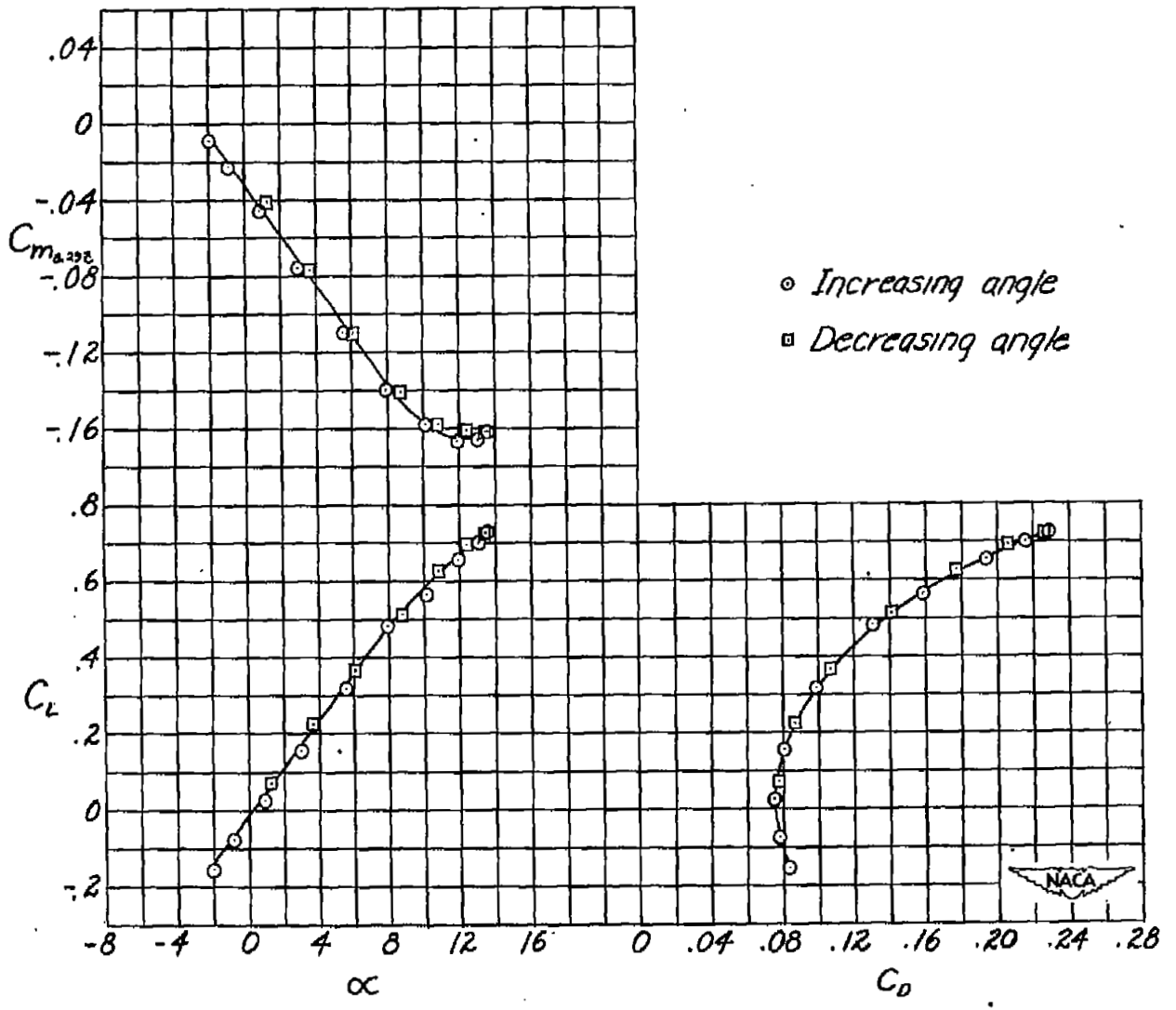

(b) Horizontal tail off..

Figure 7.- Concluded.

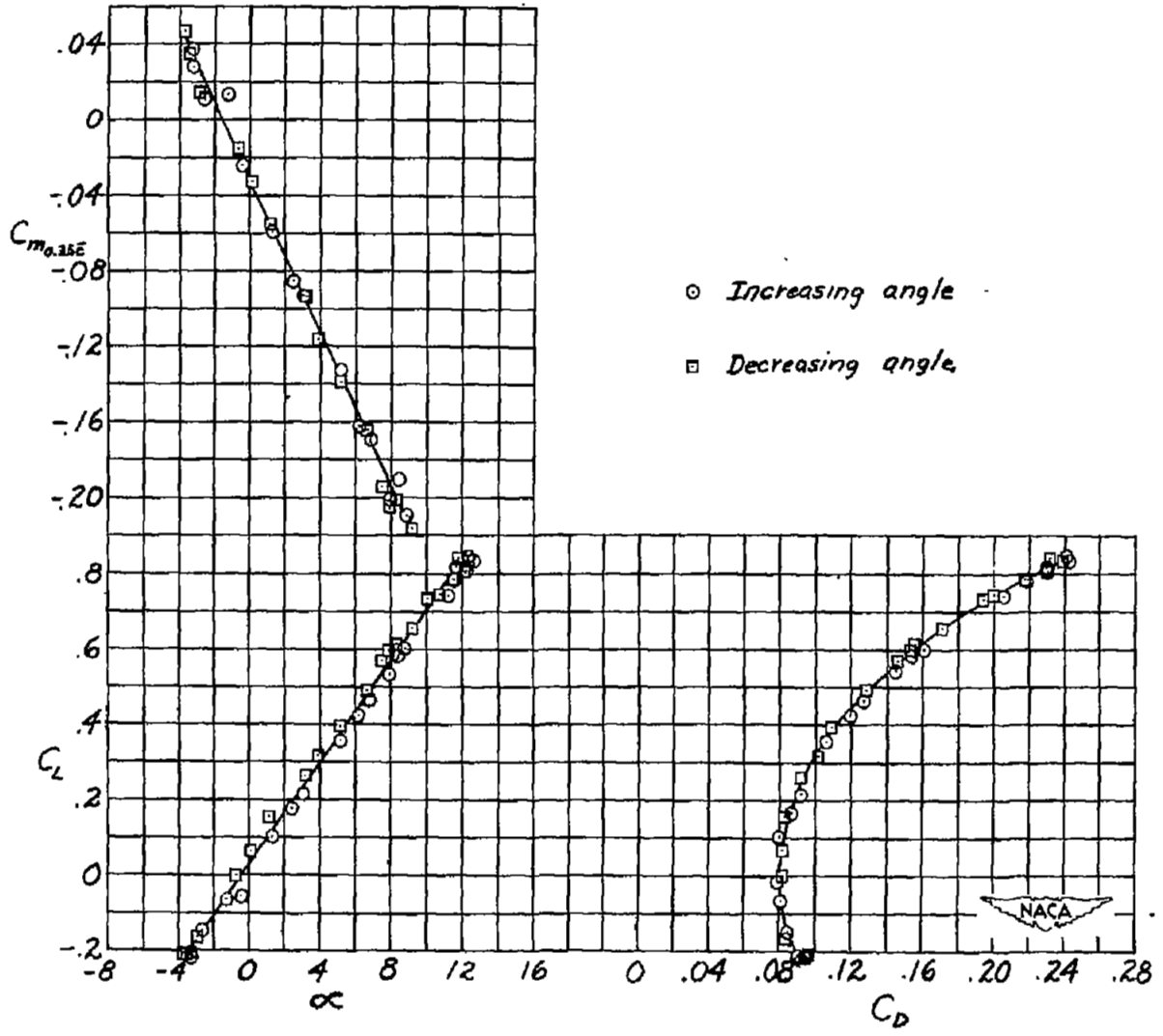

(a) $i_t = -2^\circ$.

Figure 8.- Aerodynamic characteristics of semispan model of Bell X-5 airplane; sweepback angle 40°. $M_w = 1.23$.

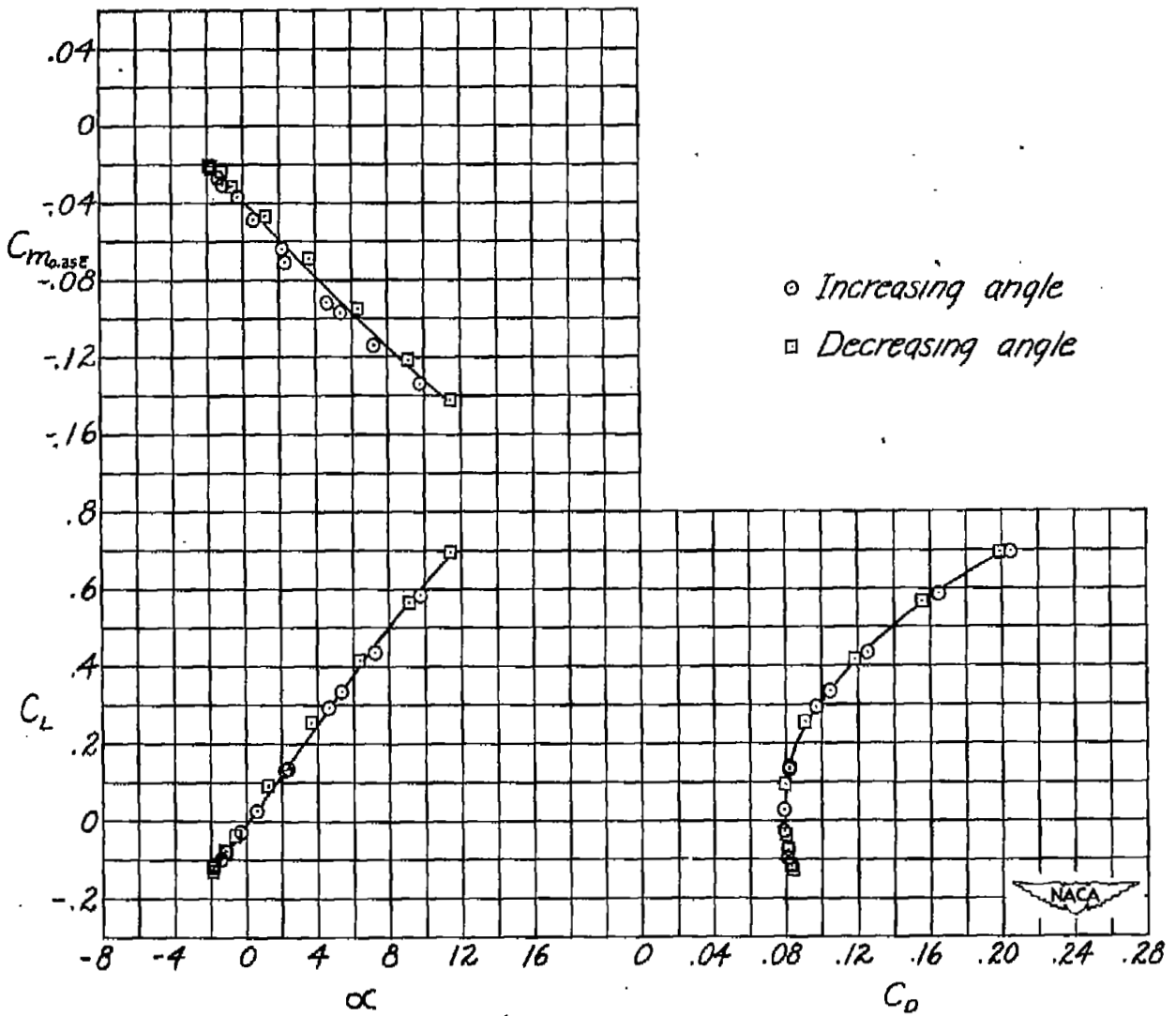

(b) Horizontal tail off.

Figure 8.- Concluded.

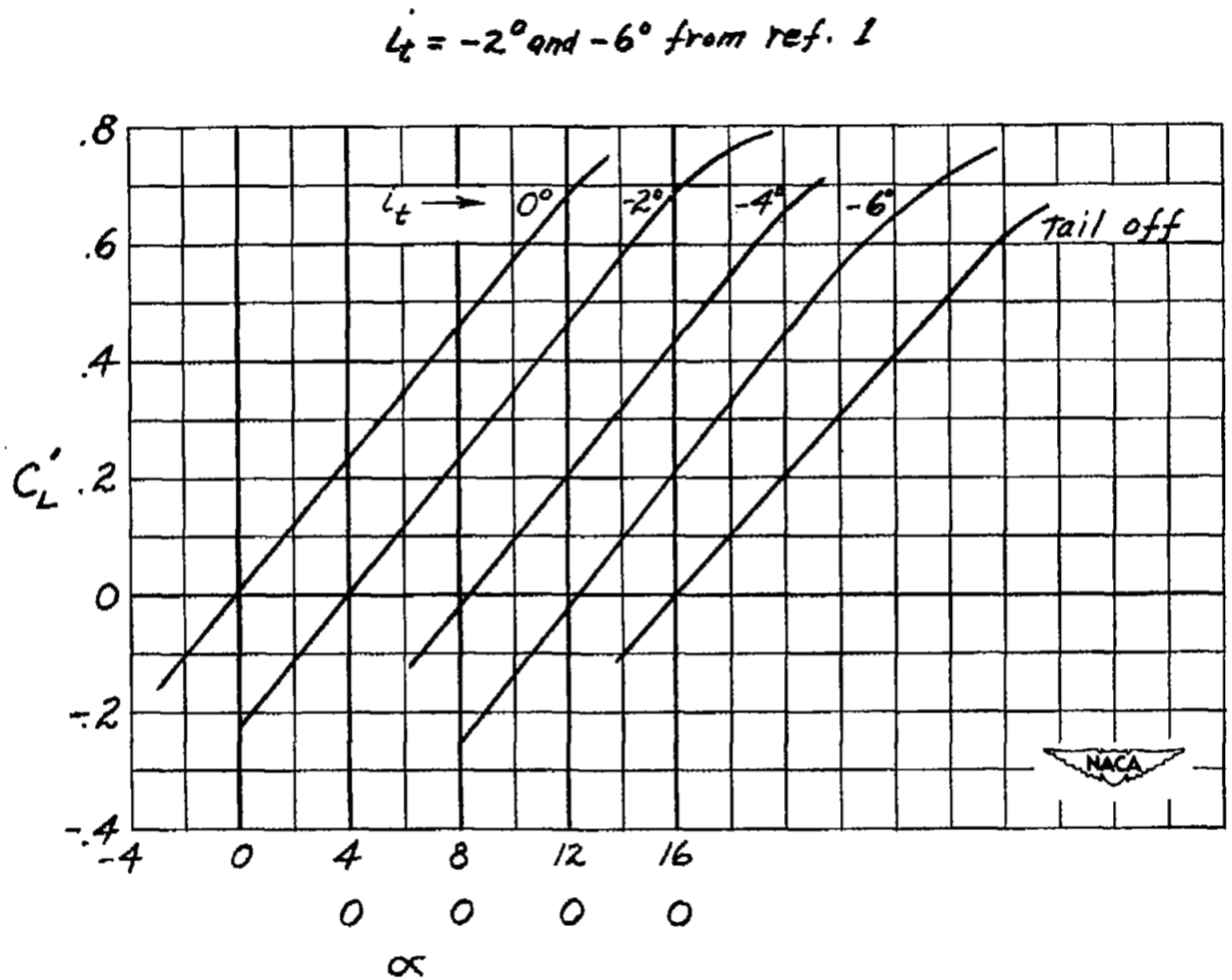

(a) $\Lambda = 60^\circ$.

Figure 9.- Variation of lift coefficient with angle of attack for several tail settings and wing sweepback angles for the semispan model of the Bell X-5 airplane. Results from references 1 and 2 also shown. (Coefficients based on 60° sweptback-wing dimensions.)

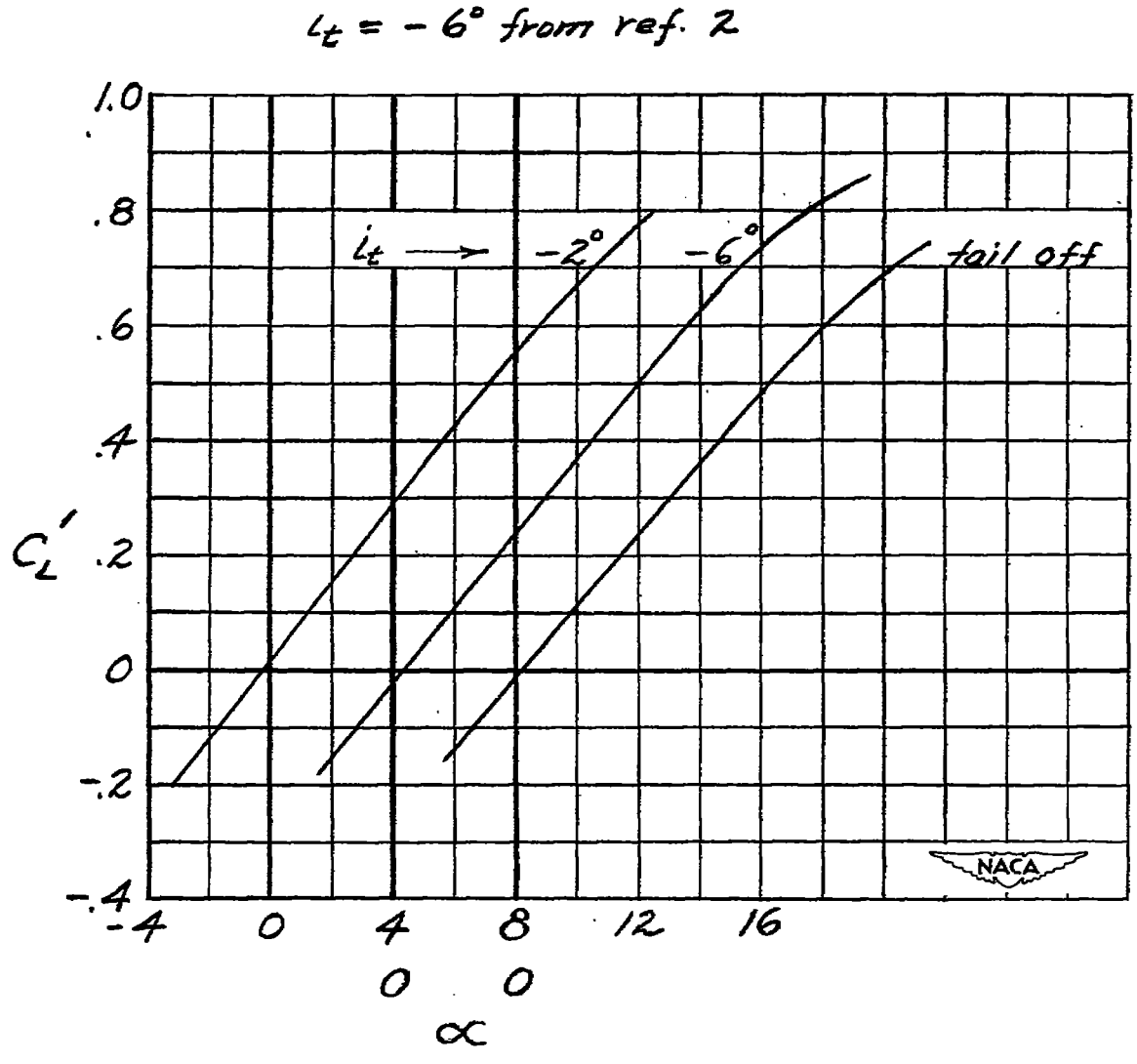

(b) $\Lambda = 50°$.

Figure 9.- Continued.

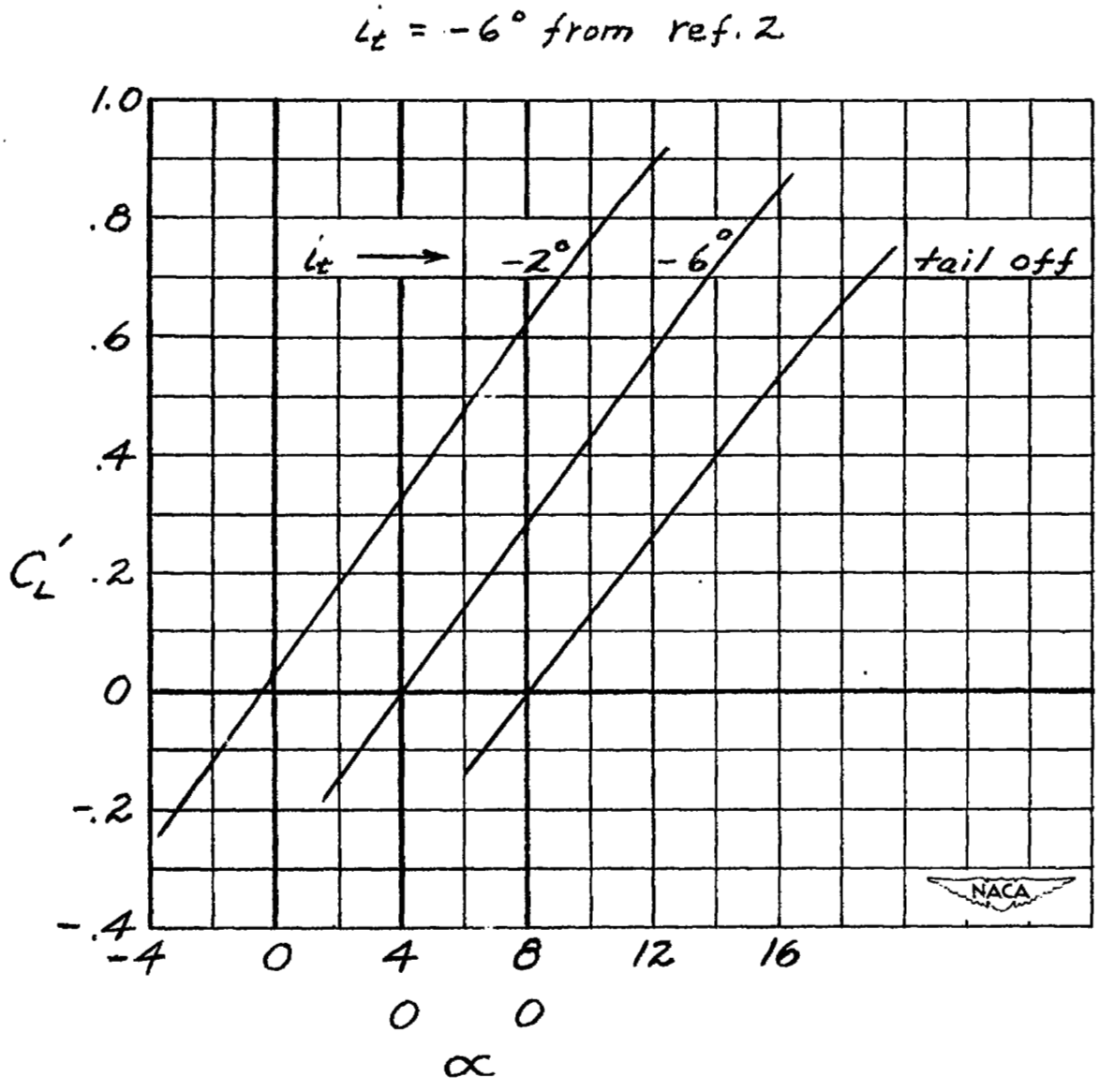

(c) $\Lambda = 40°$.

Figure 9.- Concluded.

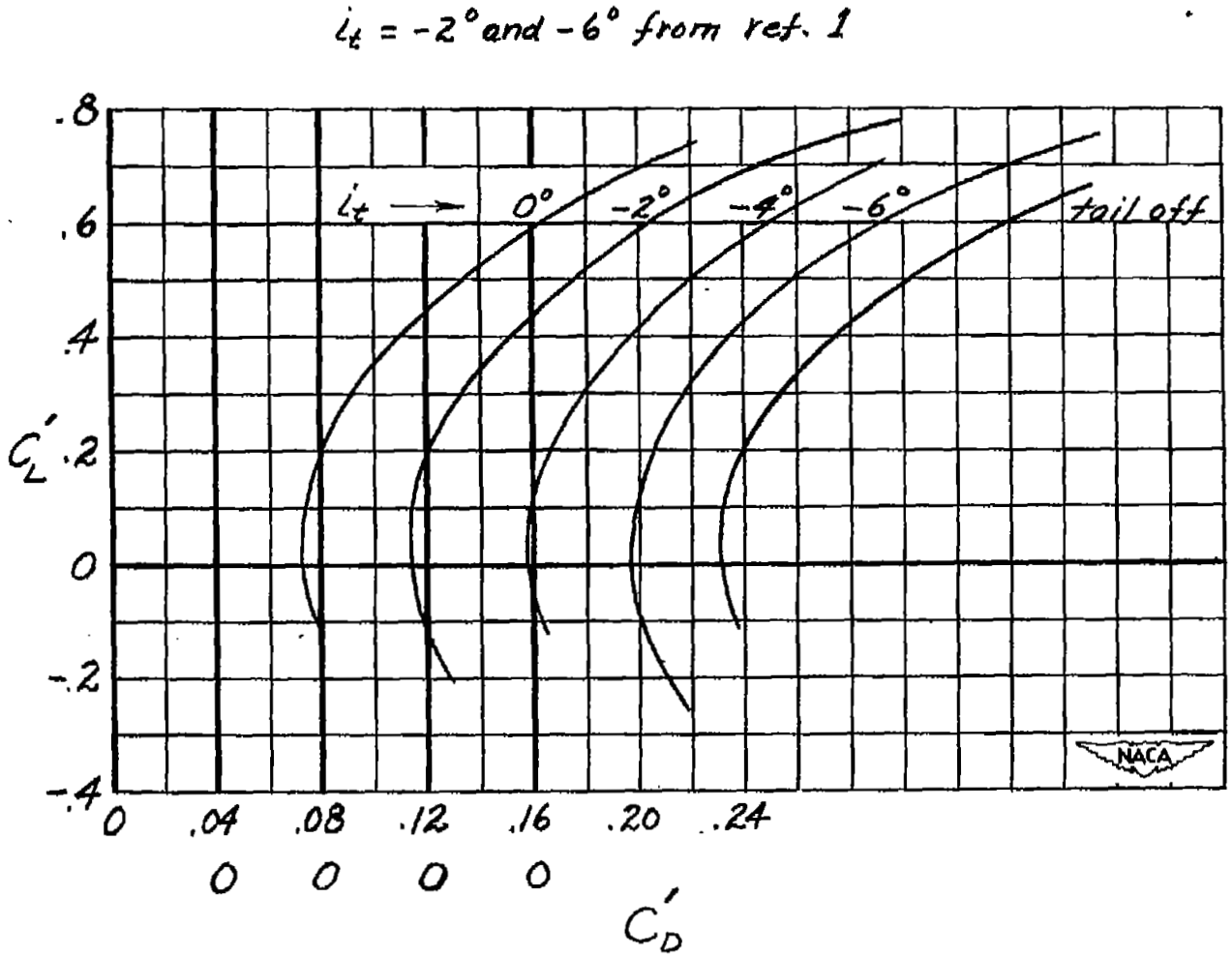

(a) $\Lambda = 60^\circ$.

Figure 10.- Variation of drag coefficient with lift coefficient for several tail settings and wing sweepback angles for the semispan model of the Bell X-5 airplane. Results from references 1 and 2 also shown. (Coefficients based on 60° sweptback-wing dimensions.)

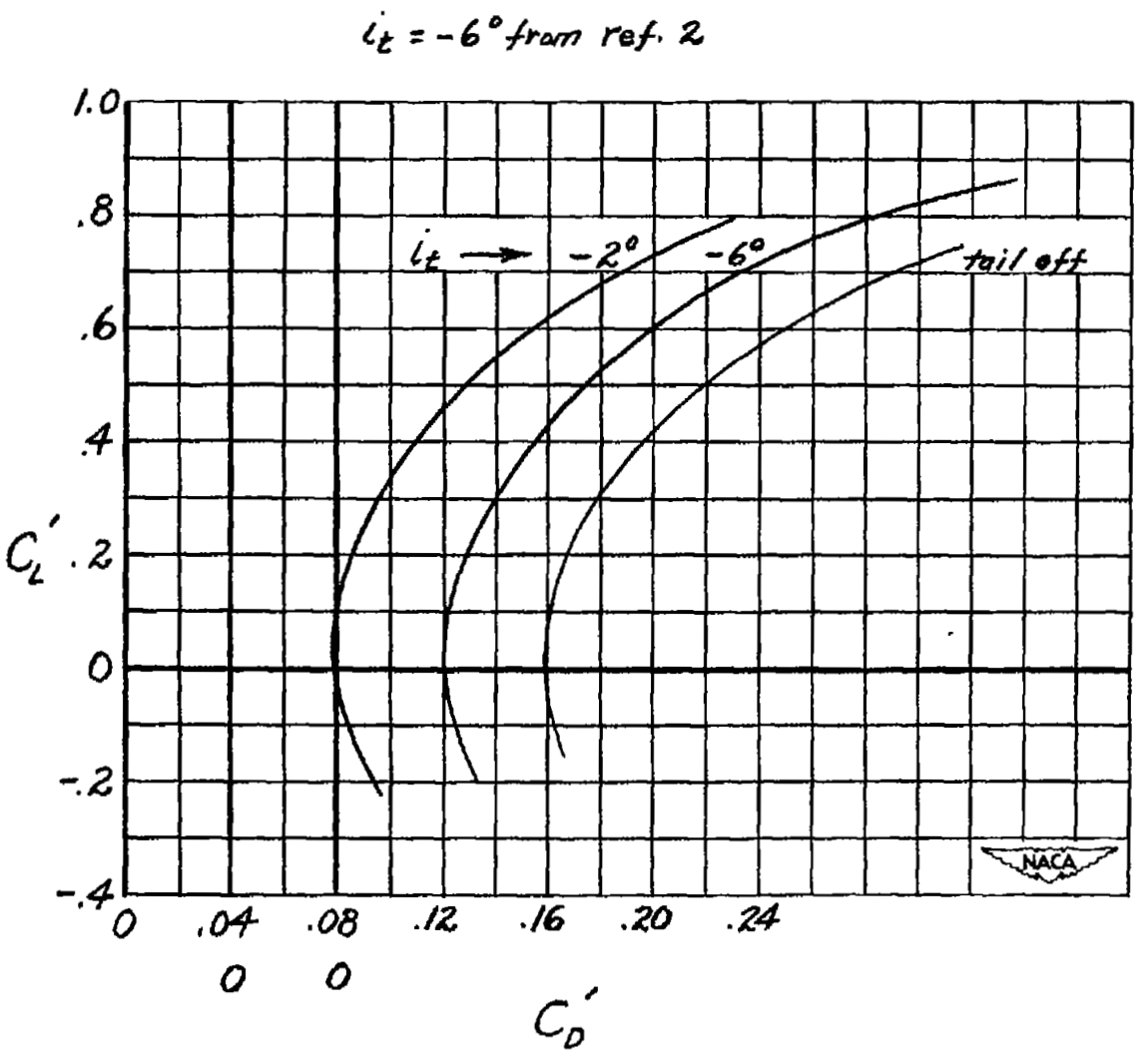

(b) $\Lambda = 50^\circ$.

Figure 10.- Continued.

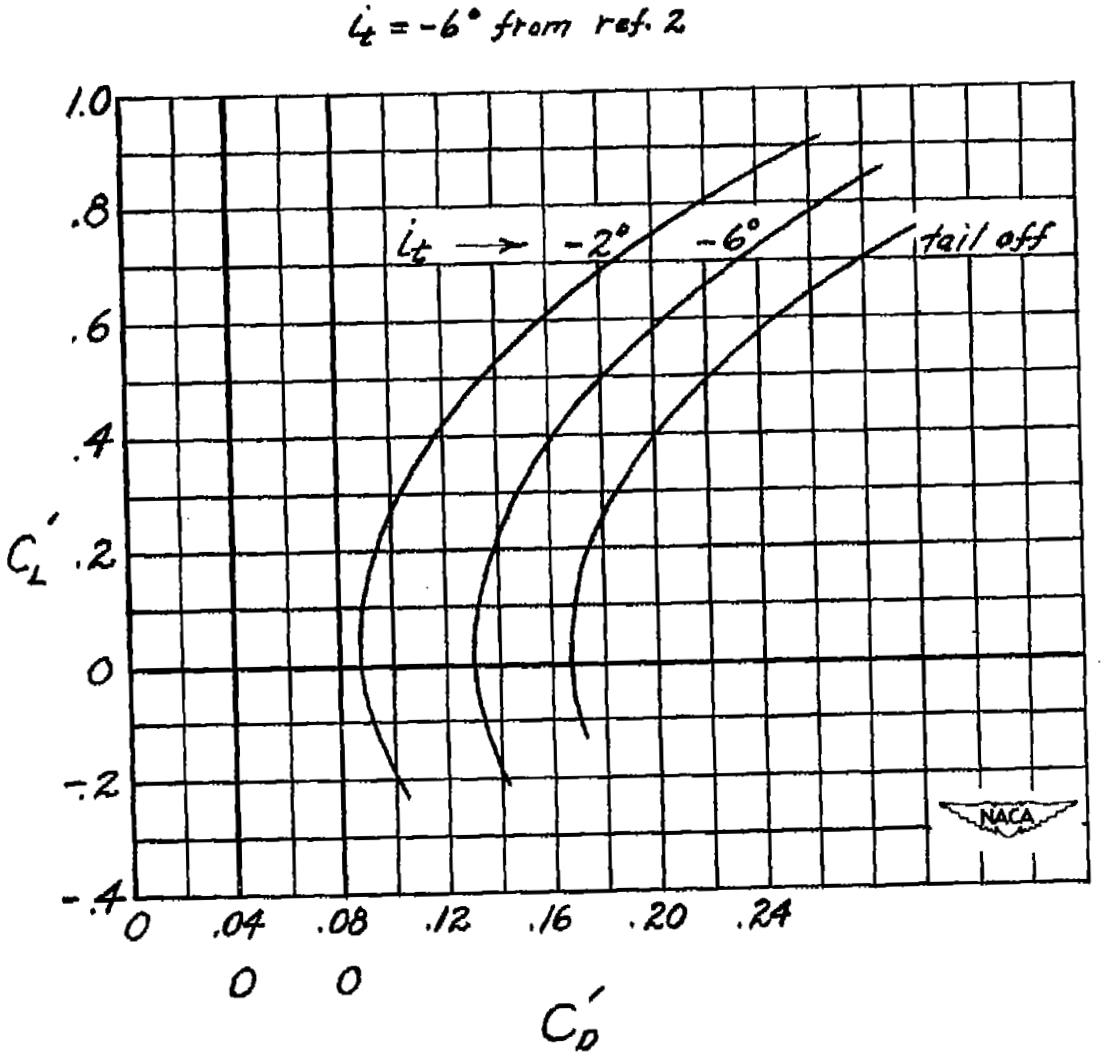

(c) $\Lambda = 40°$.

Figure 10.- Concluded.

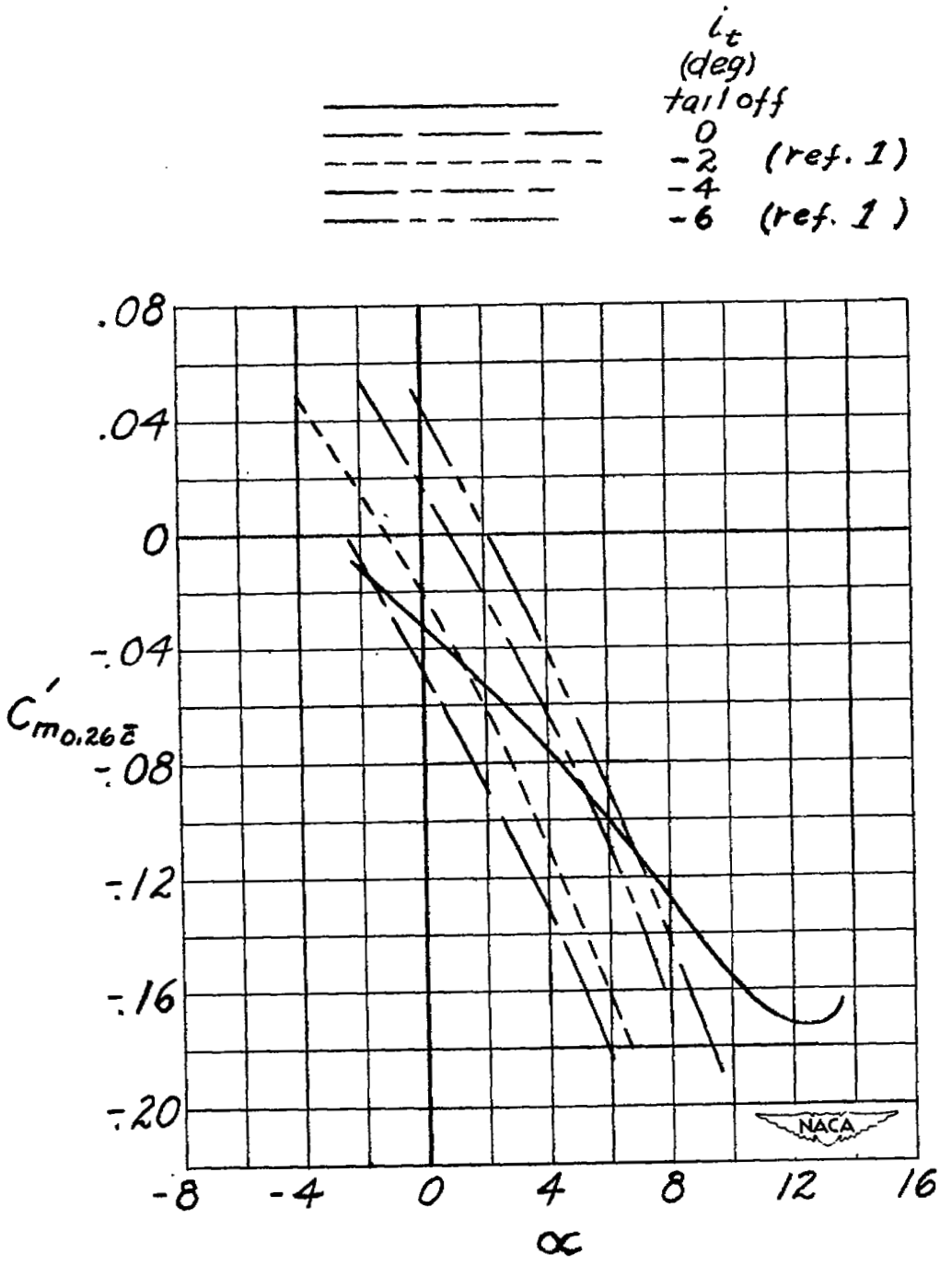

(a) $\Lambda = 60^\circ$.

Figure 11.- Variation of pitching-moment coefficient with angle of attack for several tail settings and wing sweepback angles for the semispan model of the Bell X-5 airplane. Results from references 1 and 2 also shown. (Coefficients based on 60° sweptback-wing dimensions.)

[redacted]

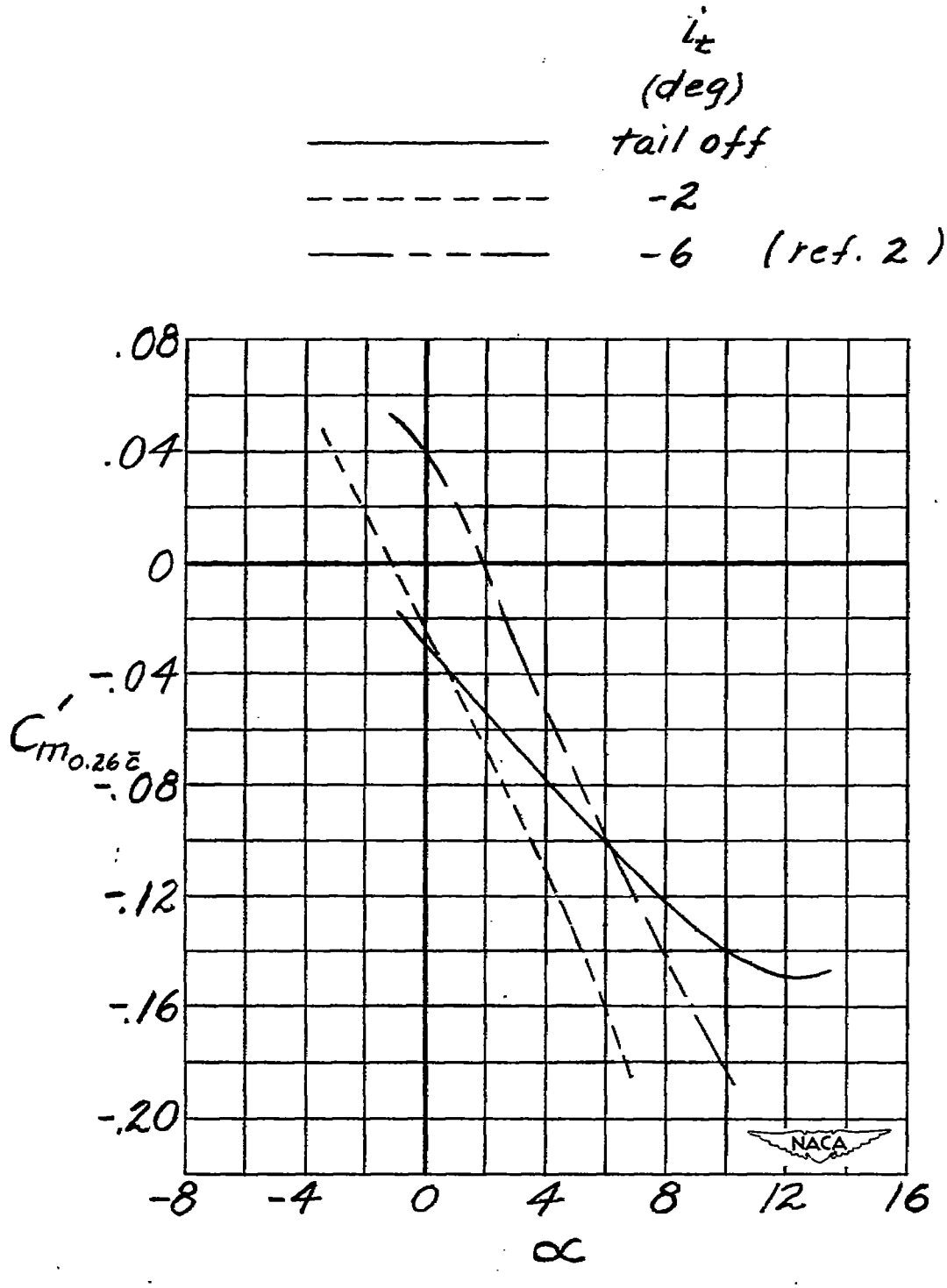

(b) $\Lambda = 50°$.

Figure 11.- Continued.

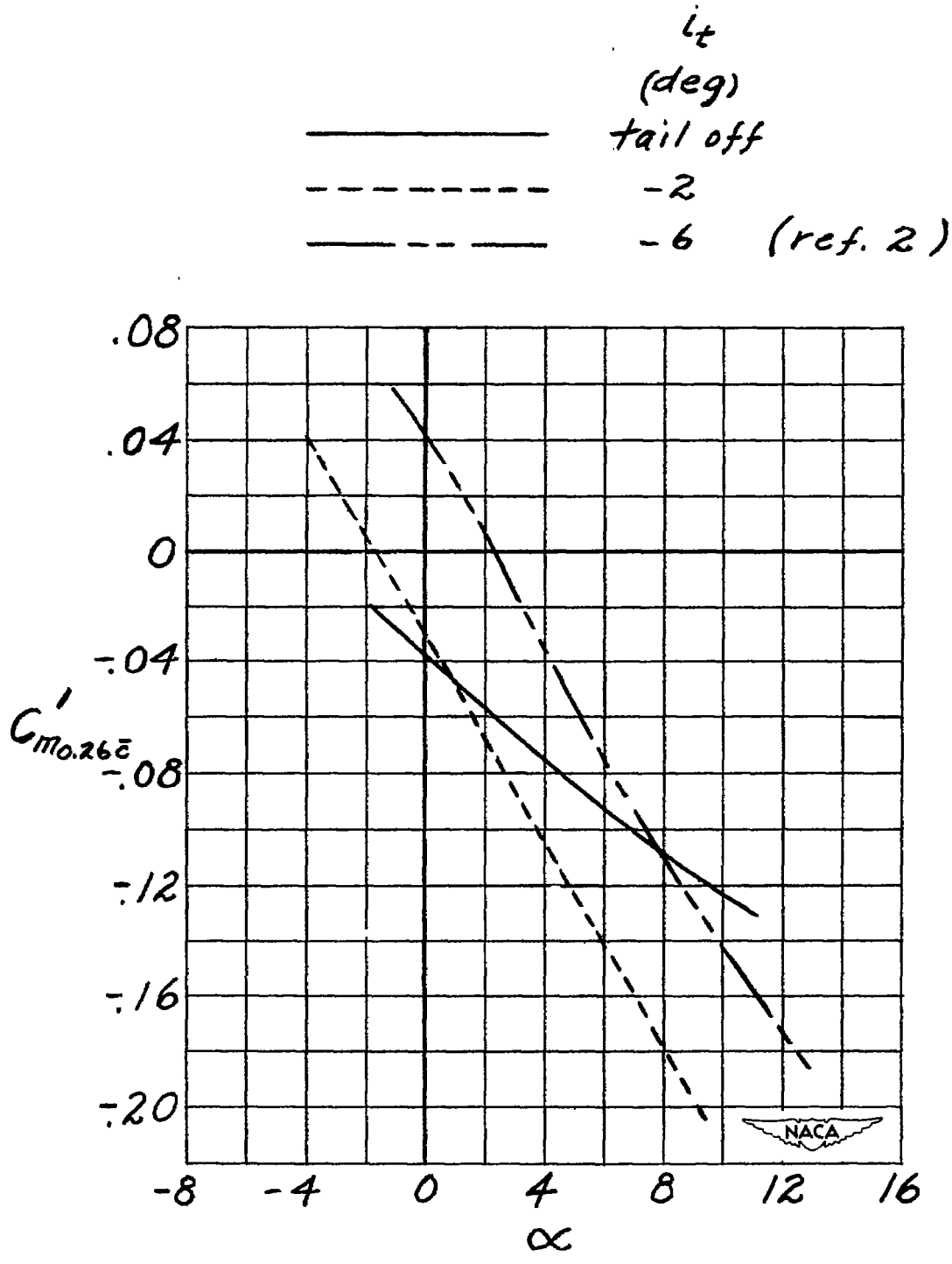

(c) $\Lambda = 40^\circ$.

Figure 11.- Concluded.

[redacted]

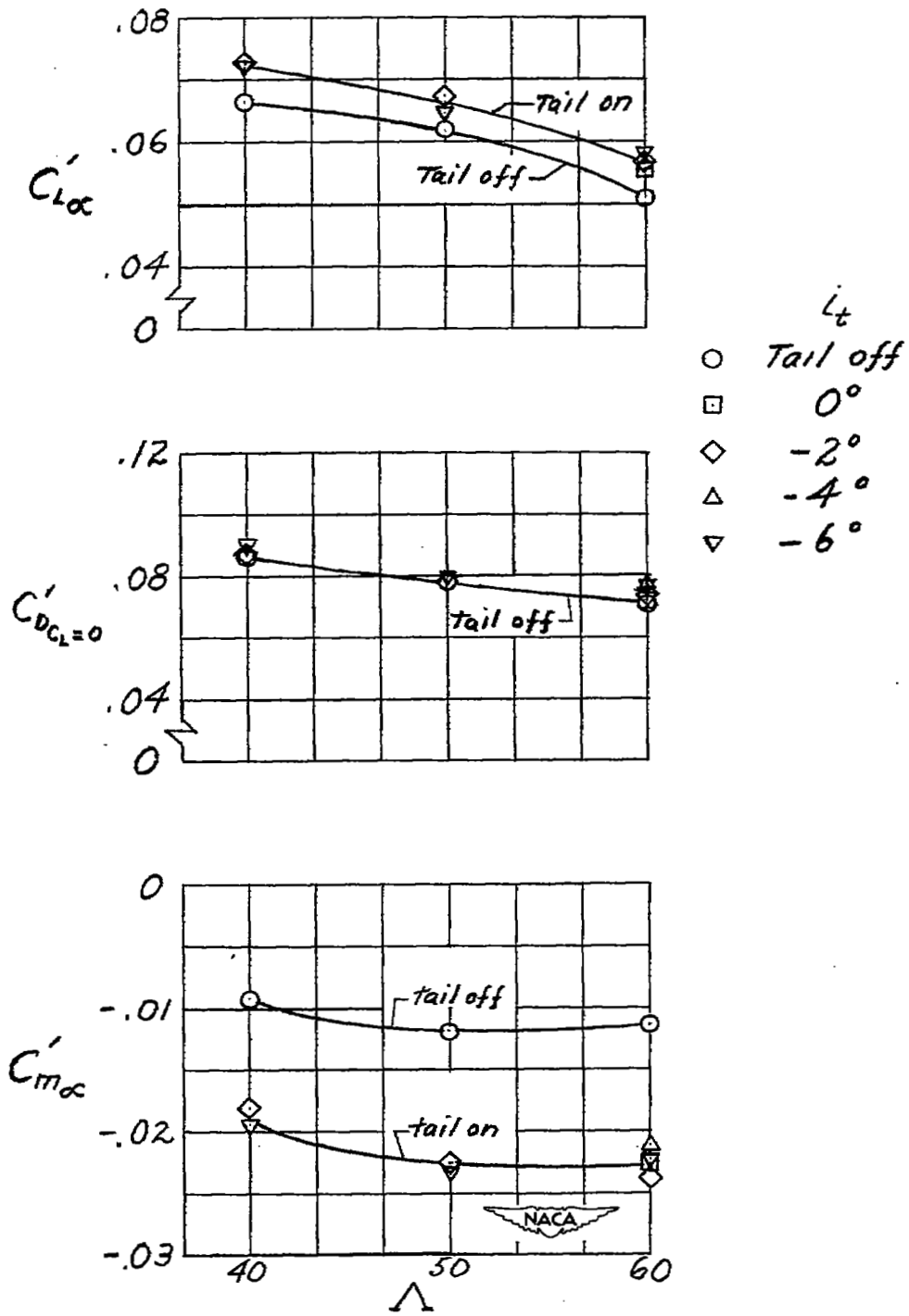

Figure 12.- Effect of sweepback angle with tail on and tail off on rate of change of lift coefficient with angle of attack, on drag coefficient at zero lift, and on rate of change of pitching-moment coefficient with angle of attack for the semispan model of the Bell X-5 airplane. (Coefficients based on 60° sweptback-wing dimensions.)

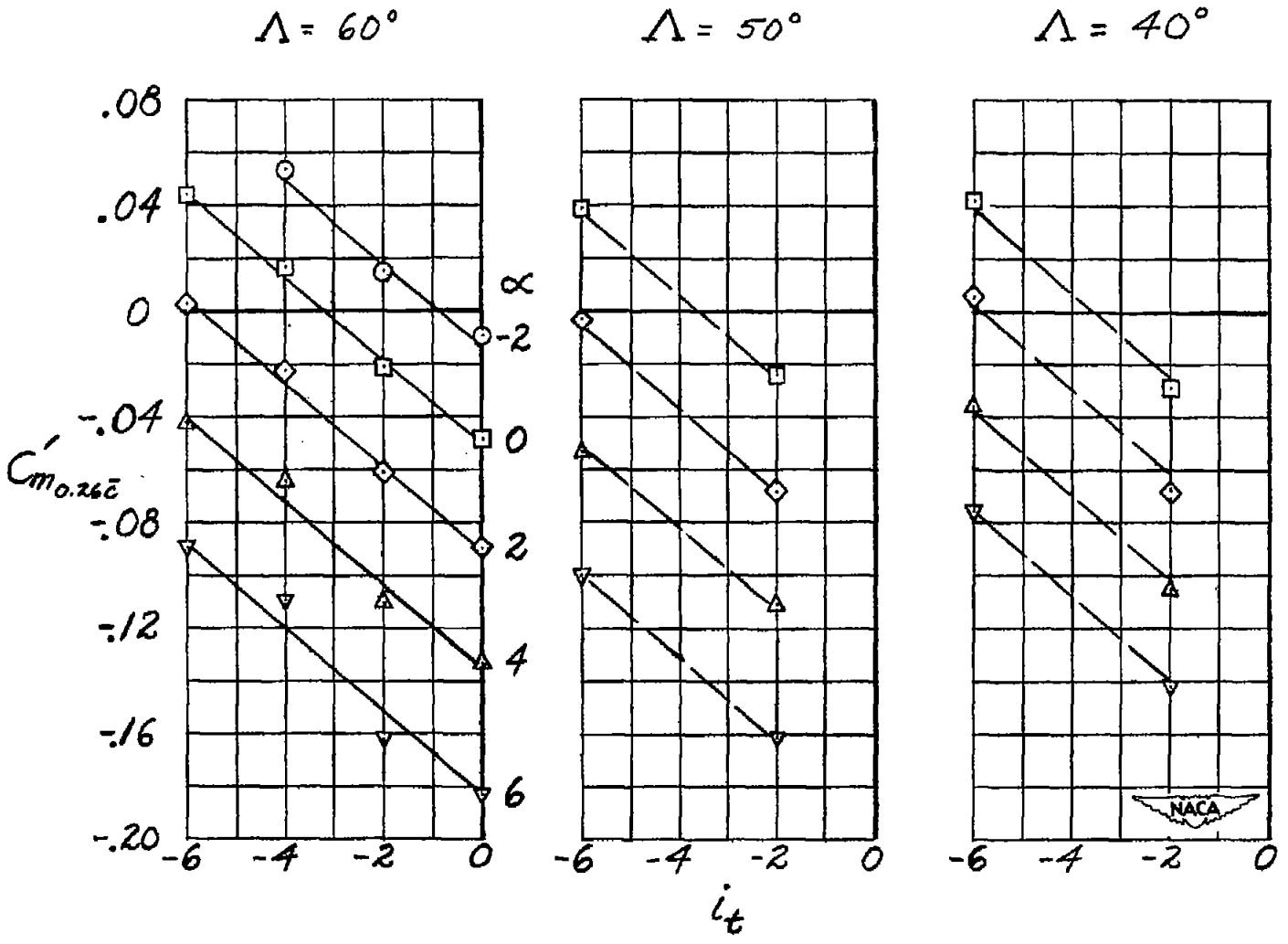

Figure 13.- Variation of pitching-moment coefficient with tail setting for several angles of attack and wing sweepback angles for semispan model of Bell X-5 airplane. (Coefficients based on 60° sweptback-wing dimensions.) Dashed lines indicate an approximate fairing due to limited number of test points.

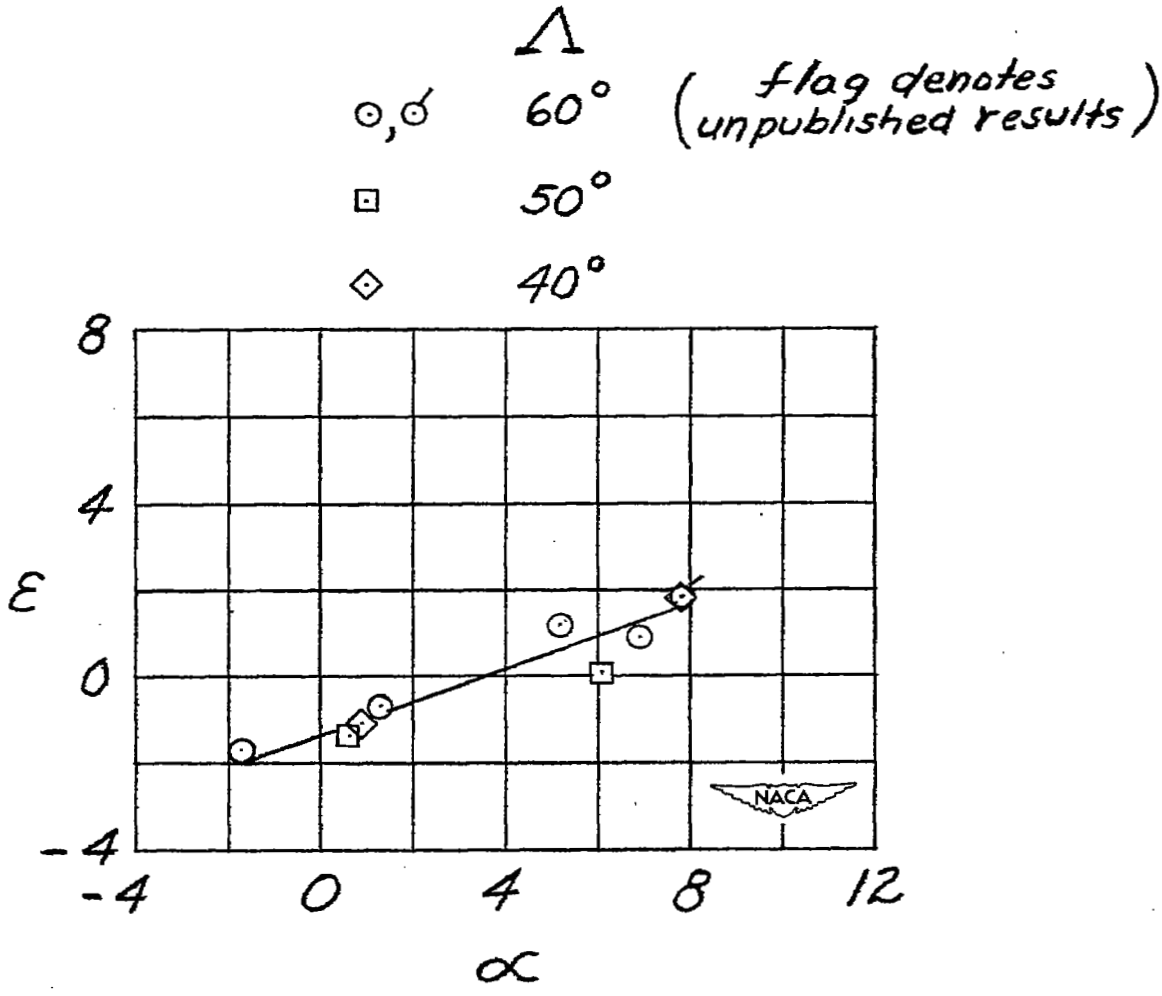

Figure 14.- Variation of downwash angle with angle of attack for several wing sweepback angles for semispan model of Bell X-5 airplane. (Coefficients based on 60° sweptback-wing dimensions.)

[redacted]